

Pattern formation for a volume-filling chemotaxis model with logistic growth ^{*}

Yazhou Han¹ Zhongfang Li¹ Jicheng Tao¹ Manjun Ma² [†]

1. Department of Mathematics, College of Science,
China Jiliang University, Hangzhou 310018, China

2. Department of Mathematics, School of Science,
Zhejiang Sci-Tech University, Hangzhou, 310018, China

June 23, 2016

Abstract

This paper is devoted to investigate the pattern formation of a volume-filling chemotaxis model with logistic cell growth. We first apply the local stability analysis to establish sufficient conditions of destabilization for uniform steady-state solution. Then, weakly nonlinear analysis with multi-scales is used to deal with the emerging process of patterns near the bifurcation point. For the single unstable mode case, we derive the Stuart-Landau equations describing the evolution of the amplitude, and thus the asymptotic expressions of patterns are obtained in both supercritical case and subcritical case. While for the case of multiple unstable modes, we also derive coupled amplitude equations to study the competitive behavior between two unstable modes through the phase plane analysis. In particular, we find that the initial data play a dominant role in the competition. All the theoretical and numerical results are in excellently qualitative agreement and better quantitative agreement than that in [1]. Moreover, in the subcritical case, we confirm the existence of stationary patterns with larger amplitudes when the bifurcation parameter is less than the first bifurcation point, which gives an positive answer to the open problem proposed in [2].

keywords: pattern formation, weakly nonlinear analysis, chemotaxis system, volume-filling, logistic growth

1 Introduction

In the fifties of last century, Turing [3] had proposed a pioneering work to explain the phenomenon of pattern formation. In [3], based on the reaction-diffusion system, Turing studied the self-organization process which can generate

^{*}The work of Yazhou Han was supported by the National Natural Science Foundation of China (Grant No. 11201443). The work of Manjun Ma Was supported by the National Natural Science Foundation of China (Grant No. 11271342), the Provincial Natural Science Foundation of Zhejiang (Grant No. LY15A010017) and the Science Foundation of Zhejiang Sci-Tech University under Grant No. 15062173-Y. The work of Jicheng Tao was supported by the Provincial Natural Science Foundation of Zhejiang (Grant No. LY16A010009).

[†]Corresponding author, Tel: +86 571 86843224, Email: mjunm9@zstu.edu.cn

some kind of ordered structures (such as zebra stripes) in the biological world. This process is usually a passive diffusion process. Meanwhile, in the biological world, there is another class of significant diffusion — active diffusion process, namely the tendency to some kind of chemical substances. The tendency is termed as *chemotaxis*, or *chemosensitive movement*. In fact, *chemotaxis* plays a great role in the lives of living organisms such as locating food, searching for mates and notifying the dangers that their companions are facing.

This paper aims to study a class of chemotaxis model with volume-filling effect and logistic cell growth, which was introduced firstly by Painter and Hillen (see [4, 5]), as follows

$$\begin{cases} \frac{\partial u}{\partial t} = \nabla(d_1 \nabla u - \chi u(1-u)\nabla v) + \mu u(1 - \frac{u}{u_c}), \\ \frac{\partial v}{\partial t} = d_2 \Delta v + \alpha u - \beta v, \end{cases} \quad (1.1)$$

where $(x, t) \in \Omega \times [0, +\infty)$, Ω is a bounded domain in \mathbb{R}^N with smooth boundary $\partial\Omega$; $u(x, t)$ is the cell density and $v(x, t)$ denotes the chemical concentration; $d_1 > 0$ and $d_2 > 0$ denote the cell and chemical diffusion coefficients, respectively; $\chi u(1-u)\nabla v$ represents the chemotactic flux under a volume constraint 1 (called crowding capacity), $\chi > 0$ is the chemotactic coefficients measuring the strength of the chemotactic response; $\mu u(1 - \frac{u}{u_c})$ is the cell kinetics term describing the logistic growth of cells with the growth rate $\mu > 0$ and carrying capacity u_c fulfilling $0 < u_c < 1$; $\alpha u - \beta v$ with $\alpha, \beta > 0$ is the dynamic term of chemical substances, αu implies that the chemical is secreted by cells themselves, βv is the degradation of chemicals. For completeness, we shall consider the system (1.1) subject to initial data

$$u(x, 0) = u_0 \geq 0, \quad v(x, 0) = v_0 \geq 0, \quad x \in \Omega, \quad (1.2)$$

and Neumann boundary condition

$$\frac{\partial u}{\partial \nu} = \frac{\partial v}{\partial \nu} = 0, \quad t > 0, x \in \partial\Omega, \quad (1.3)$$

where ν denote the outward unit normal vector on $\partial\Omega$.

The model (1.1)-(1.3) has been studied from different views by many scholars. We just outline some of them in the following paragraph. More details can be seen in [1, 2, 4–10] and references therein.

In 2009, Hillen and Painter[6] summarized the derivation of chemotaxis model and the model variations. Then, they outlined mathematical approaches for determining global existence and showed how the instability conditions depend on the parameters. Particularly, for the case $\mu = 0$, Wang and Xu[7] covered six specific cases of the chemotactic flux, and obtained the existence of patterns by globally bifurcation analysis. Moreover, if let $\frac{\chi}{d_1} \rightarrow +\infty$, Wang and Xu found that the solution of (1.1) tended to spiky or transition layer.

In 2009, for small chemotatic parameter χ , Ou and Yuan[8] proved the existence of travelling wavefronts connecting $(\bar{u}, \bar{v}) = (u_c, \frac{\alpha}{\beta} u_c)$ to $(0, 0)$, where $(u_c, \frac{\alpha}{\beta} u_c)$ and $(0, 0)$ are the only two uniform steady states to (1.1). Ma, Yang and Tang [9] generalized the result of [8] and established the existence of travelling wave solution for the general reaction terms. Recently, for the larger chemotatic parameter χ , we studied the invasion process of the pattern in the

form of a travelling wave and got the asymptotic expression of temporal-spatial pattern (see [10]).

In 2012, Ma, Ou and Wang [1] studied the steady-state solutions of the volume-filling chemotaxis model (1.1)-(1.3). They proved that (\bar{u}, \bar{v}) is globally asymptotically stable when $\chi = 0$, but if

$$\chi > \frac{\mu d_2 + \beta d_1 + 2\sqrt{d_1 d_2 \mu \beta}}{\alpha u_c(1 - u_c)} \triangleq \chi_c, \quad (1.4)$$

they gave the existence of stationary patterns by the index theory. Then, by the method of asymptotic analysis, they obtained the asymptotic expressions of stationary patterns with small amplitudes near bifurcation points and prove that, if a pattern solution with small amplitude is stable, then it must lie in the first pattern branch. However, by the method of [1], they can not obtain the specific expression of the amplitude.

In the subsequent work [2], Ma, et al. considered the case $0 < \chi < \chi_c$ and obtained the following results.

Proposition 1.1. *Let $\alpha, \beta, \mu, d_1, d_2$ be fixed and take $\Omega = [0, l]$. Then, the following statements are valid:*

(i) *If there exists some positive integer n_0 such that $n_0 = \left(\frac{\mu\beta}{d_1 d_2}\right)^{\frac{1}{4}} \frac{l}{\pi}$, then system (1.1) does not admit nonconstant steady-state solution with small amplitudes for any $\chi \in [0, \chi_c)$.*

(ii) *If $n \neq \left(\frac{\mu\beta}{d_1 d_2}\right)^{\frac{1}{4}} \frac{l}{\pi}$ for any positive integer n , then system (1.1) does not admit nonconstant steady-state solution with small amplitudes for any $\chi \in [0, \chi_c]$.*

In addition, they have proposed an open problem as follows: **whether there exist non-negative stationary pattern solutions with large amplitudes for $\chi < \chi_c$.**

In this paper, using the weakly nonlinear analysis (see [11–17] and references therein), we will derive the amplitude equation to investigate the process of pattern formation and get much more accurate expressions of pattern solutions. Moreover, we will theoretically give a positive answer to the open problem and a stationary pattern with large amplitude will be numerically presented from the full system (1.1)-(1.3) with $\chi < \chi_c$, which can be found in Subsection 3.2.2.

This paper is arranged as follows. In section 2, a class of sufficient conditions of destabilization for uniform steady-state solution will be obtained by the local stability analysis. Section 3 is devoted to study the process of pattern formation by the weakly nonlinear analysis. We first discuss the case of single unstable mode and get the cubic and quintic Stuart-Landau equation to predict the evolution of amplitude of pattern. In particularly, under the subcritical case, we compare our results with the results of [1], which show that our results are more efficient. Moreover, for the subcritical case, the bifurcation diagram of (3.24) shows the phenomenon of hysteresis and jumping. Then, the second topic discussed in Section 3 is the case of multiple unstable modes. There, we find that there exists competitive phenomenon between multiple unstable modes and the initial data play the dominant roles in the evolution of pattern solution. In section 4, we summarize the results and give some further discussion. For the completeness, four appendices, which process some specific calculation, are presented at the end of this paper.

2 Destabilization condition

In this section, we will give a class of sufficient conditions of destabilization for (\bar{u}, \bar{v}) by the local stability analysis. Let $u = \bar{u} + W^{(1)}(x, t)$, $v = \bar{v} + W^{(2)}(x, t)$. Then, we get the linearized system of (1.1) as follows

$$\dot{\mathbf{w}} = K\mathbf{w} + D^\chi \nabla^2 \mathbf{w}, \quad (2.1)$$

where

$$\mathbf{w} = \begin{pmatrix} W^{(1)} \\ W^{(2)} \end{pmatrix}, \quad K = \begin{pmatrix} -\mu & 0 \\ \alpha & -\beta \end{pmatrix}, \quad D^\chi = \begin{pmatrix} d_1 & -\chi u_c(1 - u_c) \\ 0 & d_2 \end{pmatrix}.$$

The solution with the form $\mathbf{w} = \begin{pmatrix} 1 \\ 1 \end{pmatrix} e^{i\mathbf{k} \cdot \mathbf{x} + \lambda t}$ leads to the following dispersion relation, which characterizes the relation between eigenvalue λ and the wavenumber $k = |\mathbf{k}|$,

$$\lambda^2 + g(k^2)\lambda + h(k^2) = 0, \quad (2.2)$$

where

$$g(k^2) = k^2 \text{tr}(D^\chi) - \text{tr}(K), \quad (2.3)$$

$$h(k^2) = \det(D^\chi)k^4 + qk^2 + \det(K), \quad (2.4)$$

$$q = \mu d_2 + \beta d_1 - \alpha \chi u_c(1 - u_c). \quad (2.5)$$

From the local stability theory it follows that the steady state (\bar{u}, \bar{v}) is locally stable if $\mathbf{Re}(\lambda) \leq 0$, and (\bar{u}, \bar{v}) is unstable if $\mathbf{Re}(\lambda) > 0$.

Since $g(k^2) > 0$, then (2.2) does not admit a pair of conjugate pure imaginary roots. Thus, Hopf bifurcation can not appear for the system (1.1).

To ensure that (\bar{u}, \bar{v}) loses its stability, there exists at least one eigenvalue λ satisfying $\mathbf{Re}(\lambda) > 0$. Notice that

$$\lambda = \frac{1}{2}(-g \pm \sqrt{g^2 - 4h}), \quad (2.6)$$

a class of sufficient conditions of destabilization for (\bar{u}, \bar{v}) is $h(k^2) < 0$ for some k^2 . Next we discuss the borderline case $h(k^2) = 0$.

If $h(k^2) = 0$, then

$$\chi = \frac{(\mu + d_1 k^2)(\beta + d_2 k^2)}{\alpha u_c(1 - u_c)k^2} \geq \chi_c, \quad (2.7)$$

and the equal sign holds if and only if

$$k^2 = \sqrt{\frac{\mu\beta}{d_1 d_2}} \triangleq k_c^2. \quad (2.8)$$

On the other hand, if $k^2 = -\frac{q}{2d_1 d_2}$, then

$$h_{\min} = \mu\beta - \frac{q^2}{4d_1 d_2} = \mu\beta - \frac{(\alpha \chi u_c(1 - u_c) - \mu d_2 - \beta d_1)^2}{4d_1 d_2}. \quad (2.9)$$

Thus, as presented in the Fig. 2.1, $h_{\min} = 0$ provided that $\chi = \chi_c$. If $\chi < \chi_c$, then $h_{\min} > 0$ and both of the eigenvalues of (2.2) satisfy $\mathbf{Re}(\lambda) < 0$, and thus (\bar{u}, \bar{v}) is locally asymptotically stable. If $\chi > \chi_c$, then $h_{\min} < 0$, and there exist k^2 such that (2.2) has two real eigenvalues with different signs, which leads to the destabilization of (\bar{u}, \bar{v}) .

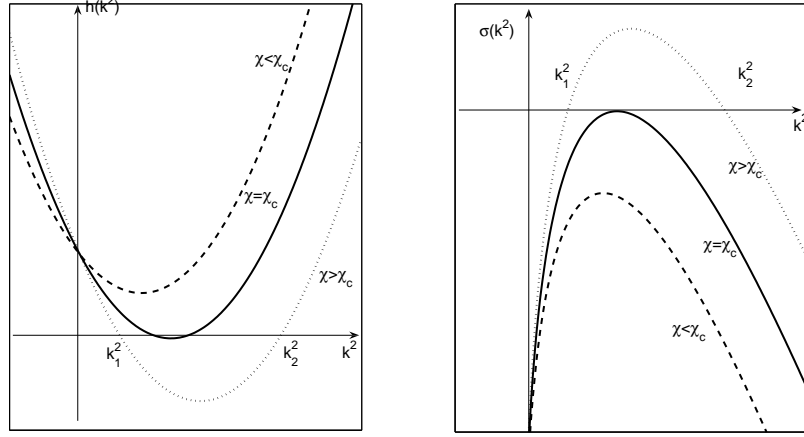


Fig. 2.1: Left: Plot of $h(k^2)$, Right: Growth rate of the k th mode.

Result 2.1 (Sufficient conditions of destabilization). *If $\chi > \chi_c$ and there exist modes k^2 such that*

$$k_1^2 < k^2 < k_2^2, \quad (2.10)$$

then uniform steady-state solution (\bar{u}, \bar{v}) destabilizes, where

$$k_1^2 = \frac{-q - \sqrt{q^2 - 4d_1d_2\mu\beta}}{2d_1d_2}, \quad (2.11)$$

$$k_2^2 = \frac{-q + \sqrt{q^2 - 4d_1d_2\mu\beta}}{2d_1d_2} \quad (2.12)$$

are the two positive roots of $h(k^2) = 0$.

In particular, when $N = 1$, $\Omega = [0, l]$, the uniform steady state (\bar{u}, \bar{v}) destabilizes provided that $\chi > \chi_c$ and there exists at least a positive integer n_0 such that

$$k_1^2 < \left(\frac{n_0\pi}{l}\right)^2 < k_2^2.$$

In the following, through the weakly nonlinear analysis, we shall study how the solutions evolve into stationary patterns when $\chi > \chi_c$ and χ is close to χ_c . Additionally, the discuss of this paper focuses on the case of one dimension and the higher dimensional case will be presented in the subsequent work. So, we assume that $N = 1$ and $\Omega = [0, l]$ in the sequel.

3 Asymptotic expression for stationary pattern

3.1 Weakly nonlinear analysis

Let

$$\mathbf{w} = \begin{pmatrix} W^{(1)} \\ W^{(2)} \end{pmatrix} = \begin{pmatrix} u - \bar{u} \\ v - \bar{v} \end{pmatrix}, \quad (3.1)$$

and then the system (1.1) can be rewritten as follows

$$\mathbf{w}_t = \mathcal{L}^\chi \mathbf{w} + \mathcal{N} \mathcal{L}^\chi \mathbf{w}, \quad (3.2)$$

where

$$\mathcal{L}^\chi = K + D^\chi \frac{\partial^2}{\partial x^2},$$

$$\mathcal{N} \mathcal{L}^\chi \mathbf{w} = \begin{pmatrix} -\chi \frac{\partial}{\partial x} ((1 - 2u_c) W^{(1)} \frac{\partial W^{(2)}}{\partial x} - (W^{(1)})^2 \frac{\partial W^{(2)}}{\partial x}) - \frac{\mu}{u_c} (W^{(1)})^2 \\ 0 \end{pmatrix}.$$

Expand χ , \mathbf{w} and t as

$$\chi = \chi_c + \varepsilon \chi_1 + \varepsilon^2 \chi_2 + \varepsilon^3 \chi_3 + \varepsilon^4 \chi_4 + \varepsilon^5 \chi_5 + \dots, \quad (3.3)$$

$$\mathbf{w} = \varepsilon \mathbf{w}_1 + \varepsilon^2 \mathbf{w}_2 + \varepsilon^3 \mathbf{w}_3 + \varepsilon^4 \mathbf{w}_4 + \varepsilon^5 \mathbf{w}_5 + \dots, \quad (3.4)$$

$$t = t(T_1, T_2, T_3, \dots), \quad T_i = \varepsilon^i t, i = 1, 2, \dots, \quad (3.5)$$

where $\mathbf{w}_i = (W_i^{(1)}, W_i^{(2)})^T$, and $T_i, i = 1, 2, \dots$ represent different time scales. Substituting (3.3), (3.4) and (3.5) into (3.2) and collecting the terms at each order in ε , we obtain a sequence of coefficient equations.

$O(\varepsilon)$:

$$\mathcal{L}^{\chi_c} \mathbf{w}_1 = 0, \quad (3.6)$$

$O(\varepsilon^2)$:

$$\mathcal{L}^{\chi_c} \mathbf{w}_2 = \mathbf{F} = \begin{pmatrix} F^{(1)} \\ F^{(2)} \end{pmatrix} = \begin{pmatrix} F^{(1)} \\ \frac{\partial W_1^{(2)}}{\partial T_1} \end{pmatrix}, \quad (3.7)$$

$O(\varepsilon^3)$:

$$\mathcal{L}^{\chi_c} \mathbf{w}_3 = \mathbf{G}, \quad (3.8)$$

where

$$\begin{aligned} F^{(1)} &= \frac{\partial W_1^{(1)}}{\partial T_1} + \chi_1 u_c (1 - u_c) \frac{\partial^2 W_1^{(2)}}{\partial x^2} \\ &+ \chi_c \frac{\partial}{\partial x} ((1 - 2u_c) W_1^{(1)} \frac{\partial}{\partial x} W_1^{(2)}) + \frac{\mu}{u_c} (W_1^{(1)})^2. \end{aligned} \quad (3.9)$$

The explicit expression of G and all the detailed calculation are given in Appendix A.

3.2 Stationary pattern for single unstable mode

Firstly, we assume that k_c^2 is the unique unstable mode satisfying (2.10). So, the solution to the equation (3.6) with the Neumann boundary conditions is

$$\mathbf{w}_1 = A \rho \cos(k_c x), \quad (3.10)$$

where the amplitude function A only depends on temporal variable and

$$\rho = \begin{pmatrix} M \\ 1 \end{pmatrix} = \begin{pmatrix} \frac{\beta + k_c^2 d_2}{\alpha} \\ 1 \end{pmatrix} \in \text{Ker}(K - k_c^2 D^\chi). \quad (3.11)$$

Substituting \mathbf{w}_1 into (3.7) leads to

$$\mathbf{F} = \left[\frac{\partial A}{\partial T_1} \rho - A \begin{pmatrix} 0 & k_c^2 \chi_1 u_c (1 - u_c) \\ 0 & 0 \end{pmatrix} \rho \right] \cos(k_c x) - \left(M \chi_c k_c^2 (1 - 2u_c) - \frac{\mu M^2}{2u_c} \right) A^2 \cos(2k_c x) + \left(\frac{\mu M^2}{2u_c} \right) A^2. \quad (3.12)$$

Suppose that

$$\mathbf{w}^* = \psi \cos(k_c x) \quad \text{with } \psi = \begin{pmatrix} M^* \\ 1 \end{pmatrix}, \quad (3.13)$$

is a fundamental solution of $L^* \mathbf{w}^* = 0$, where L^* is the adjoint operator of L^{χ_c} , $M^* = \frac{\alpha}{\mu + d_1 k_c^2}$. By the solvability condition for (3.7), we have $\langle \mathbf{F}, \mathbf{w}^* \rangle = 0$, and then obtain

$$\frac{\partial A}{\partial T_1} = \gamma A \quad \text{with } \gamma = \frac{k_c^2 \chi_1 (u_c - u_c^2) M^*}{1 + M M^*}. \quad (3.14)$$

Noting that the solution $A = C \exp(\gamma T_1)$ of (3.14) can not predict correctly the evolution of amplitude, we take $\frac{\partial A}{\partial T_1} = 0$ and $\chi_1 = 0$ simply to satisfy the solvability condition. Particularly, $\frac{\partial A}{\partial T_1} = 0$ means that solution is independent of time scale T_1 , i.e. $\frac{\partial \mathbf{w}}{\partial T_1} = 0$.

Then, from (3.7) and (3.12) it follows that (3.7) has solution

$$\mathbf{w}_2 = A^2 \mathbf{W}_{20} + A^2 \mathbf{W}_{22} \cos(2k_c x), \quad (3.15)$$

where

$$\mathbf{W}_{20} = \begin{pmatrix} -\frac{M^2}{2u_c} \\ -\frac{\alpha M^2}{2\beta u_c} \end{pmatrix}, \quad \mathbf{W}_{22} = \begin{pmatrix} \frac{\beta + 4k_c^2 d_2}{\alpha} \\ 1 \end{pmatrix} \mathbf{W}_{22}^{(2)}, \quad (3.16)$$

$$\mathbf{W}_{22}^{(2)} = \frac{\alpha \left(\frac{\mu M^2}{2u_c} - \chi_c k_c^2 M (1 - 2u_c) \right)}{4\alpha k_c^2 \chi_c u_c (1 - u_c) - (\mu + 4k_c^2 d_1)(\beta + 4k_c^2 d_2)}. \quad (3.17)$$

To explore the evolution of the amplitude A , we further discuss the third-order coefficient equation (3.8). Substituting \mathbf{w}_1 and \mathbf{w}_2 into (3.8) and combining with the solvability condition $\langle \mathbf{G}, \mathbf{w}^* \rangle = 0$, we get the cubic Stuart-Landau equation of amplitude A as follows

$$\frac{dA}{dT_2} = \sigma A - L A^3, \quad (3.18)$$

where

$$\sigma = \frac{\langle G_{11}, \psi \rangle}{\langle \rho, \psi \rangle} = \frac{k_c^2 \chi_2 (u_c - u_c^2) M^*}{1 + M M^*} > 0, \quad (3.19)$$

$$L = \frac{\langle G_{13}, \psi \rangle}{\langle \rho, \psi \rangle} = \frac{G_{13}^{(1)} M^*}{1 + M M^*}, \quad (3.20)$$

$$G_{13}^{(1)} = \chi_c (2u_c - 1) k_c^2 (W_{20}^{(1)} + M W_{22}^{(2)} - \frac{1}{2} W_{22}^{(1)}) + \frac{1}{4} \chi_c M^2 k_c^2 + \frac{\mu M}{u_c} (2W_{20}^{(1)} + W_{22}^{(1)}). \quad (3.21)$$

The detailed computations of (3.15) and (3.18) can be found in Appendix B.

Obviously, the dynamics of (3.18) can be divided into two cases according to the sign of L , i.e., the supercritical case and the subcritical case corresponding to $L > 0$ and $L < 0$, respectively. By (3.20), the sign of L completely depends on that of $G_{13}^{(1)}$. Especially, when $u_c = \frac{1}{2}$, we have

$$\begin{aligned} G_{13}^{(1)} &= \frac{1}{4}\chi_c M^2 k_c^2 - 4\mu M^3 \\ &\quad + \frac{2\mu^2 M^3 (\beta + 4k_c^2 d_2)}{4k_c^2 \alpha \chi_c u_c (1 - u_c) - (\mu + 4k_c^2 d_1)(\beta + 4k_c^2 d_2)} \\ &= \sqrt{\mu} \left\{ \frac{1}{4}\chi_c M^2 \sqrt{\frac{\beta}{d_1 d_2}} - 4\sqrt{\mu} M^3 \right. \\ &\quad \left. + \frac{2\mu^{\frac{3}{2}} M^3 (\beta + 4k_c^2 d_2)}{k_c^2 \alpha \chi_c - (\mu + 4k_c^2 d_1)(\beta + 4k_c^2 d_2)} \right\}. \end{aligned} \quad (3.22)$$

Thus, we can obtain the following conclusion.

Result 3.1. *Let $u_c = \frac{1}{2}$ and other parameters d_1 , d_2 , α and β be fixed. Then, if the cell growth rate μ is small enough, then (3.18) is supercritical; while μ is large enough, then (3.18) is subcritical.*

In the following, we shall derive the amplitude equation in both supercritical case and subcritical bifurcation case.

3.2.1 The supercritical case

Because of $\sigma > 0$ and $L > 0$, it is easy to know that (3.18) has a globally asymptotic stable solution

$$A_\infty \triangleq \sqrt{\frac{\sigma}{L}},$$

which represents the limit value of the amplitude A . Substituting A_∞ into (3.4), (3.10) and (3.15), we have the second-order asymptotic expression of the stationary pattern as follows

$$\mathbf{w} = \varepsilon \rho \sqrt{\frac{\sigma}{L}} \cos(k_c x) + \varepsilon^2 \frac{\sigma}{L} (\mathbf{w}_{20} + \mathbf{w}_{22} \cos(2k_c x)) + O(\varepsilon^3). \quad (3.23)$$

In Fig.3.1, a numerical example is presented to show the comparison between the numerical solution of (1.1)-(1.3) and the weakly nonlinear asymptotic solution (3.23). Since $k_c \neq \frac{n\pi}{l}$ for any positive integer n , in (3.23) we replace k_c by $\overline{k}_c = 3.5$, i.e., the first unstable mode when χ passes the critical value χ_c . It is observed from Fig.3.1 that both the wave number and the amplitude are in perfectly agreement between the numerical solution of (1.1)-(1.3) and the approximation (3.23) for the cases $\varepsilon = 0.1$ and $\varepsilon = 0.2$.

Remark 3.2. If there is no $n \in N_+$ such that $k_c = \frac{n\pi}{l}$ for $\chi = \chi_c$, then we replace k_c by the first admissible mode $\overline{k}_c = \frac{n_0\pi}{l}$ in (3.10) and (3.15), where n_0 satisfies $\chi_0(n_0) = \chi_{\min}$ with

$$\chi_{\min} = \min_n \left\{ \chi_0(n) = \frac{(d_1(\frac{n\pi}{l})^2 + \mu)(\beta + d_2(\frac{n\pi}{l})^2)}{\alpha u_c(1 - u_c)(\frac{n\pi}{l})^2}, n = 1, 2, \dots \right\}.$$

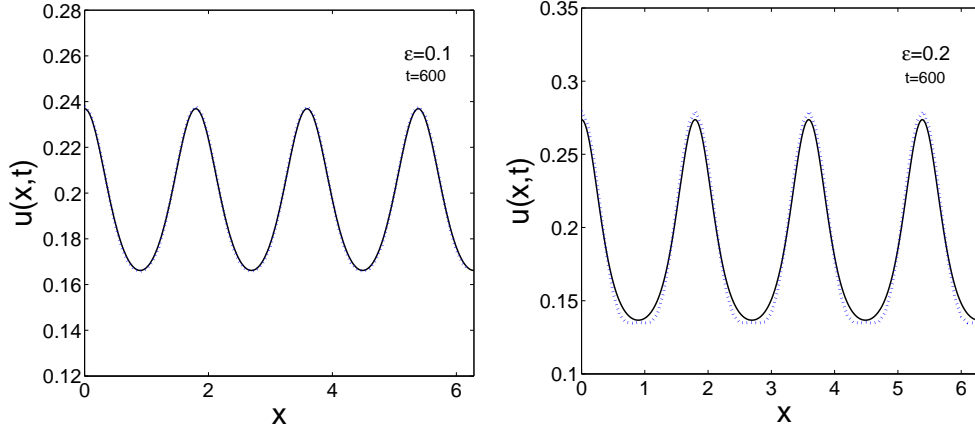


Fig. 3.1: Comparison between the weakly nonlinear solution (dashed line) and the numerical solution of (1.1)-(1.3)(solid line). The initial data is set as 1% random small perturbation of the $(u_c, \frac{\alpha}{\beta}u_c)$ and the parameters are $\alpha = 36, \beta = 34, \mu = 0.5, u_c = 0.2, d_1 = 0.2, d_2 = 0.6, l = 2\pi$. With these parameters one has $\chi_c = 1.7286, k_c = 3.45$ and the first admissible unstable mode is $\bar{k}_c = 3.5$.

Here χ_{\min} is the same as that in page 753 of [1]. Accordingly, the critical value χ_c is replaced by the first bifurcation value χ_{\min} . On the other hand, we note that the second-order weakly nonlinear asymptotic solution (3.23) is consistent with that obtained in [1]. But in [1] the amplitude was not explicitly expressed by the cubic Stuart-Landau equation (3.18). So we improve the related results to the reference [1].

Remark 3.3. If $\mu = 0$, then

$$k_c = \frac{n_0\pi}{l} = 0$$

with $n_0 = 0$. Obviously there is no pattern formation. Thus, when $\mu = 0$, the bifurcation parameter χ should start with χ_{\min} .

3.2.2 The subcritical case

If $\sigma > 0$ and $L < 0$, it is easy to know that cubic Stuart-Landau equation (3.18) is not able to capture the amplitude of the pattern. Therefore, we need to push the weakly nonlinear expansion to higher order.

Performing the weakly nonlinear expansion up to $O(\varepsilon^5)$, we can get the quintic Stuart-Landau equation for the amplitude as follows

$$\frac{dA}{dT} = \bar{\sigma}A - \bar{L}A^3 + \bar{Q}A^5, \quad (3.24)$$

where

$$\bar{\sigma} = \sigma + \varepsilon^2\tilde{\sigma}, \quad \bar{L} = L + \varepsilon^2\tilde{L}, \quad \bar{Q} = \varepsilon^2\tilde{Q}, \quad (3.25)$$

σ and L are given in (3.19) and (3.20), respectively; and $\tilde{\sigma}, \tilde{L}$ and \tilde{Q} are given in (C.6). The detailed calculations are given in Appendix C.

In the subcritical case, namely $\bar{\sigma} > 0$ and $\bar{L} < 0$, and when $\bar{Q} < 0$, it is easy to check that (3.24) has a globally asymptotic stable solution

$$\bar{A}_\infty = \sqrt{\frac{\bar{L} - \sqrt{\bar{L}^2 - 4\bar{\sigma}\bar{Q}}}{2\bar{Q}}},$$

which is the limit value of amplitude A . Substituting \bar{A}_∞ into $\mathbf{w}_1, \mathbf{w}_2, \mathbf{w}_3, \mathbf{w}_4$, we obtain the following fourth-order weakly nonlinear asymptotic expression of the stationary pattern

$$\begin{aligned} \mathbf{w} &= \varepsilon \mathbf{w}_1 + \varepsilon^2 \mathbf{w}_2 + \varepsilon^3 \mathbf{w}_3 + \varepsilon^4 \mathbf{w}_4 + O(\varepsilon^5) \\ &= \bar{A}_\infty \rho \cos(k_c x) + \varepsilon^2 \bar{A}_\infty^2 (\mathbf{W}_{20} + \mathbf{W}_{22} \cos(2k_c x)) \\ &\quad + \varepsilon^3 [(\bar{A}_\infty \mathbf{W}_{31} + \bar{A}_\infty^3 \mathbf{W}_{32}) \cos(k_c x) + \bar{A}_\infty^3 \mathbf{W}_{33} \cos(3k_c x)] \\ &\quad + \varepsilon^4 [\bar{A}_\infty^2 \mathbf{W}_{40} + \bar{A}_\infty^4 \mathbf{W}_{41} + (\bar{A}_\infty^2 \mathbf{W}_{42} + \bar{A}_\infty^4 \mathbf{W}_{43}) \cos(2k_c x) \\ &\quad + \bar{A}_\infty^4 \mathbf{W}_{44} \cos(4k_c x)] + O(\varepsilon^5), \end{aligned} \quad (3.26)$$

where ρ is given in (3.11), \mathbf{W}_{20} and \mathbf{W}_{22} are given in (3.16), \mathbf{W}_{31} , \mathbf{W}_{32} and \mathbf{W}_{33} are given in (C.2), and \mathbf{W}_{40} , \mathbf{W}_{41} , \mathbf{W}_{42} , \mathbf{W}_{43} and \mathbf{W}_{44} are given in (C.4).

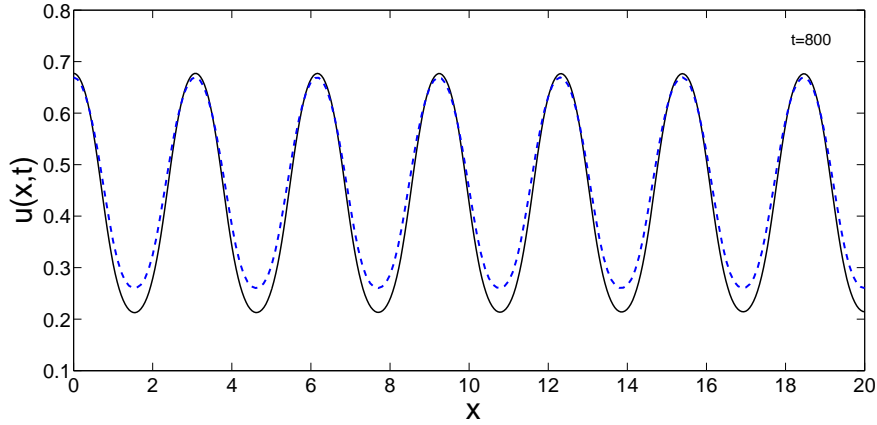


Fig. 3.2: Comparison between the weakly nonlinear solution (dashed line) and the numerical solution of (1.1)-(1.3) (solid line) with $\varepsilon = 0.1$, where the initial data is same as in Fig. 3.1 and the parameters are $\alpha = 10$, $\beta = 10$, $\mu = 0.5$, $u_c = 0.5$, $d_1 = 0.3$, $d_2 = 1$, $l = 20$. In this case, $\chi_c = 2.3798$, $k_c = 2.0205$.

Fig.3.2 shares the same parameters as that in Fig. 4 of [1]. We have $\bar{\sigma} = 1.5351$, $\bar{L} = -0.7588$ and $\bar{Q} = -0.6415$. And then, the equation (3.24) has a stable equilibrium $\bar{A}_\infty = 1.4992$. we see that in Fig.3.2 the analytical approximation and the numerical simulation are in qualitative and quantitative agreement better than Fig.4 of [1].

With the parameters in Fig.3.2, we plot the bifurcation diagram Fig.3.3 of (3.24). In Fig. 3.3, there exist two turning points χ_c and χ_s , where χ_s is the zero point of the discriminant of the equilibrium equation of (3.24), i.e. χ_s is the root of $\bar{L}^2 - 4\bar{\sigma}\bar{Q} = 0$. In figure 3.3, we numerically get

$$\chi_c = 2.3798, \quad \chi_s = 2.3728.$$

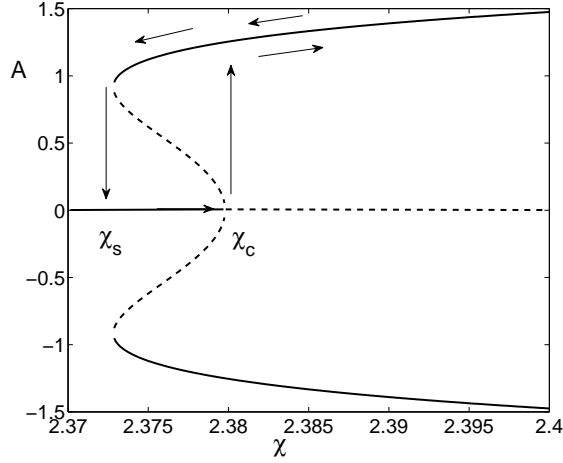


Fig. 3.3: The bifurcation diagram of (3.24). The parameter values are the same as that in Figure 3.2

Specifically, Fig.3.3 implies the following information. the origin is locally stable for $\chi < \chi_c$, and when $\chi = \chi_c$, two backward unstable branches are generated from the origin. Decreasing χ until $\chi = \chi_s < \chi_c$, these unstable branches turn around and become stable. Thus, two stable branches coexists in the range $\chi_s < \chi < \chi_c$.

The coexisting phenomenon indicates that solutions will be hysteresis in the range $\chi_s < \chi < \chi_c$ and jump rapidly at the two values $\chi = \chi_s$ and $\chi = \chi_c$. Specifically, for any given small perturbation around $(u_c, \frac{\alpha}{\beta}u_c)$, the solution approaches asymptotically to $(u_c, \frac{\alpha}{\beta}u_c)$ if $\chi < \chi_c$; while for $\chi > \chi_c$, the solution will jump rapidly to the stable equilibrium with large amplitude. Similarly, for the stable branch with larger amplitudes, there exist the hysteresis and the jumping phenomenon at the value $\chi = \chi_s$.

Moreover, the coexisting phenomenon implies that there are stationary patterns with larger amplitudes when the bifurcation parameter $\chi \in (\chi_s, \chi_c)$. This gives an affirmative answer to the open problem proposed in [2]. A numerical example is presented in Fig. 3.4.

3.3 Stationary pattern for double unstable modes

As presented in Fig. 3.5, when ε is small, there exists only one mode such that $h(k^2) < 0$. Then, \bar{k}_c is just the most unstable mode. For this case, the asymptotic expressions of stationary pattern are discussed in the above Section. While, for larger ε , the parameter χ has a larger deviation from χ_c , there will be more than one modes satisfy $h(k^2) < 0$. We shall study how the unstable modes interact and how to determine the shape of stationary pattern.

We first analyze how the most unstable mode change. Denote the positive eigenvalue of (2.6) as λ^+ , and then

$$\lambda^+(k^2) = \frac{1}{2}(-g + \sqrt{g^2 - 4h}).$$

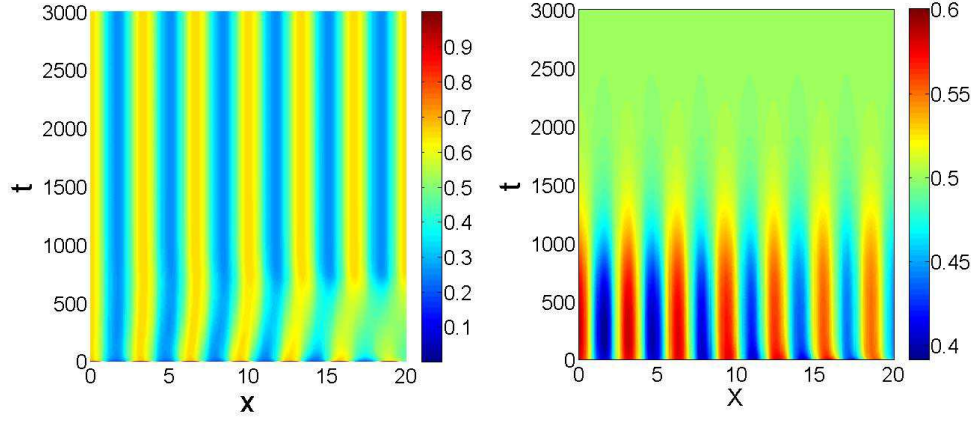


Fig. 3.4: two stable steady states \mathbf{w} expressed by (3.26) and $(u_c, \frac{\alpha}{\beta}u_c)$ coexist. The parameters are the same as that in Fig. 3.2 and $\chi = 2.3760 \in (\chi_s, \chi_c)$. Left: Pattern \mathbf{w} reached by giving the initial value $u_0 = u_c + 0.5 \cos(2x)$. Right: the uniform steady state $(u_c, \frac{\alpha}{\beta}u_c)$ reached by giving the initial value $u_0 = u_c + 0.1 \cos(2x)$.

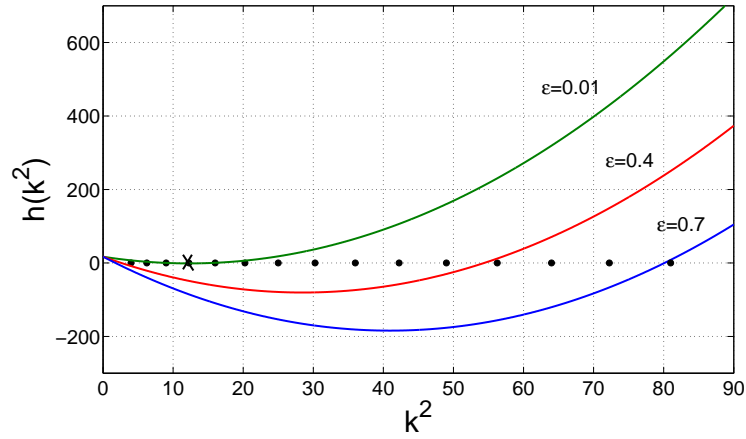


Fig. 3.5: The unstable modes are the integers and semi-integers (marked with dots) for which $h(k^2) < 0$. The critical mode \bar{k}_c is marked with a cross. The parameters are same as Fig. 3.1.

Combining the method in [18], we know that the solution k_m^2 of

$$\frac{d\lambda^+}{d(k^2)} = 0 \quad (3.27)$$

maximizes the growth rate λ^+ . Thus k_m is the wave number of the most unstable mode. Substituting $\chi = \chi_c(1 + \varepsilon^2)$ and $k_m^2 = k_c^2 + \delta$ into (3.27), we have

$$\delta = \frac{-B - \sqrt{B^2 - 4AC}}{2A} - k_c^2, \quad (3.28)$$

where

$$\begin{aligned} A &= -(d_1 - d_2)^2 d_1 d_2 < 0, \\ B &= 4d_1 d_2 q - 2d_1 d_2 (d_1 + d_2)(\mu + \beta) < 0, \\ C &= q^2 - (d_1 + d_2)(\mu + \beta)q + (d_1 + d_2)^2 \mu \beta > 0, \\ q &= -\varepsilon^2(\mu d_2 + \beta d_1) - 2(1 + \varepsilon^2)\sqrt{\mu \beta d_1 d_2} < 0. \end{aligned}$$

Noting that $\delta = 0$ if $\varepsilon = 0$ and $\frac{d\delta}{d(\varepsilon^2)} > 0$ if $\varepsilon > 0$, so we know that, with the increasing of χ , the most unstable mode k_m^2 will move away from k_c^2 . Numerical examples are given in Fig. 3.6.

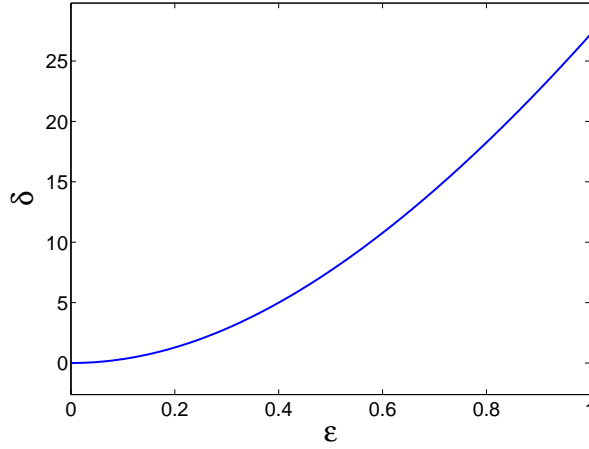


Fig. 3.6: The curve of $\frac{d\lambda^+}{d(k^2)} = 0$, where the parameters are chosen as in Fig. 3.1.

Then, we will investigate the competitive law between two unstable modes k_1 and k_2 by deriving their amplitude equations. Set the solution of (3.6) as

$$\mathbf{w}_1 = \sum_{l=1}^2 A_l \rho_l \cos(k_l x), \quad (3.29)$$

where A_l depending only on temporal variable is the amplitude of mode k_l and

$$\rho_l = \begin{pmatrix} M_l \\ 1 \end{pmatrix} \quad \text{with } M_l = \frac{\beta + k_l^2 d_2}{\alpha}, \quad l = 1, 2.$$

Applying the Fredholm alternative to (3.7) and (3.8) and repeating the process establishing the amplitude equation (3.18), we obtain the following ODE model

$$\begin{cases} \frac{dA_1}{dT} = \sigma_1 A_1 - L_1 A_1^3 - \Omega_1 A_1 A_2^2, \\ \frac{dA_2}{dT} = \sigma_2 A_2 - L_2 A_2^3 - \Omega_2 A_2 A_1^2. \end{cases} \quad (3.30)$$

The detailed calculations are given in Appendix D. Therefore, the first-order asymptotic expression of the stationary pattern is as follows

$$\mathbf{w} = \varepsilon(\rho_1 A_{1\infty} \cos(k_1 x) + \rho_2 A_{2\infty} \cos(k_2 x)) + O(\varepsilon^2), \quad (3.31)$$

where $(A_{1\infty}, A_{2\infty})$ is some stable stationary state of the system (3.30).

Since a complete analysis of the stationary points of (3.30) is too involved, therefore we just present a numerical study of a typical case. Now, the values of parameters are chosen the same as in Fig. 3.1 except $\varepsilon = 0.4$. Then, the solution of (3.27) is about $k_m^2 = (4.1105)^2$. So, we choose two unstable modes $k_1 = 4$ and $k_2 = 3.5$. By Appendix D, we have

$$\begin{aligned} \sigma_1 &= 3.3680, & L_1 &= 41.2467, & \Omega_1 &= 75.1183, \\ \sigma_2 &= 2.7532, & L_2 &= 28.1224, & \Omega_2 &= 62.0933 \end{aligned}$$

and the four non-negative equilibria

$$(0, 0), \quad (0, 0.3129), \quad (0.2858, 0), \quad (0.1995, 0.1475).$$

A further calculation leads to the corresponding Jacobian matrices as follows

$$\begin{aligned} J_{(0,0)} &= \begin{pmatrix} 3.3680 & 0 \\ 0 & 2.7532 \end{pmatrix}, & J_{(0,0.3129)} &= \begin{pmatrix} -3.9862 & 0 \\ 0 & -5.5065 \end{pmatrix}, \\ J_{(0.2858,0)} &= \begin{pmatrix} -6.7359 & 0 \\ 0 & -2.3170 \end{pmatrix}, & J_{(0.1995,0.1475)} &= \begin{pmatrix} -3.1898 & -4.4202 \\ -3.6538 & -1.5529 \end{pmatrix}. \end{aligned}$$

Therefore, $(0, 0)$ is an unstable node, $(0.1995, 0.1475)$ is a saddle point, and $(0, 0.3129)$ and $(0.2858, 0)$ are stable nodes. These can also be observed in the phase diagram in Fig. 3.7. So, the model (3.30) with these values is competitive and the system can evolve toward one of the two semi-trivial stable states $(A_1, 0) = (0.2858, 0)$ and $(0, A_2) = (0, 0.3129)$. If we take the initial data $(0.144, 0.228)$, which corresponds to the point P in Fig 3.7 and lies in the basin of attraction of the equilibrium $(0, A_2)$, then the asymptotic expression of stationary pattern is

$$u = u_c + \varepsilon A_2 M_2 \cos(k_2 x) + O(\varepsilon^2). \quad (3.32)$$

The detailed comparison between numerical solution of (1.1)-(1.3) and expected solution (3.32) is presented in Fig 3.8. While for the initial data $Q(0.344, 0.108)$ belonging the basin of attraction of the equilibrium $(A_1, 0)$ (see Fig 3.7), the asymptotic expression of the stationary pattern is changed into

$$u = u_c + \varepsilon A_1 M_1 \cos(k_1 x) + O(\varepsilon^2). \quad (3.33)$$

The comparison between (3.33) and the simulation solution of (1.1)-(1.3) is given in Fig 3.9.

It is seen that, after a long time evolution, the mode with the sufficiently dominant initial data can extinguish the other one. Thus, nonlinear effect makes the initial data play a critical role in the competition of unstable modes.

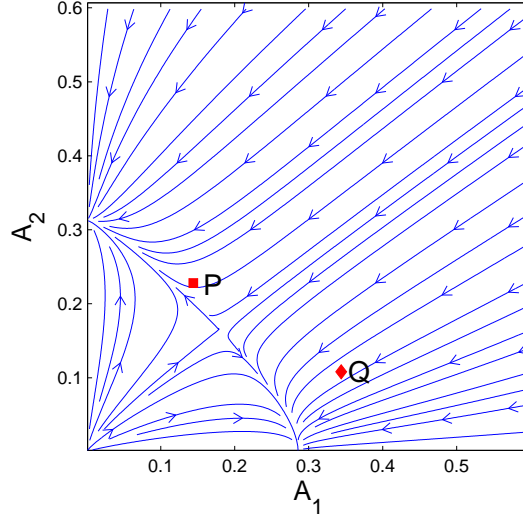


Fig. 3.7: The phase portrait of the competitive model (3.30) for modes $k_1 = 4$ and $k_2 = 3.5$. The parameters are the same as that in Fig. 3.1 except $\varepsilon = 0.4$.

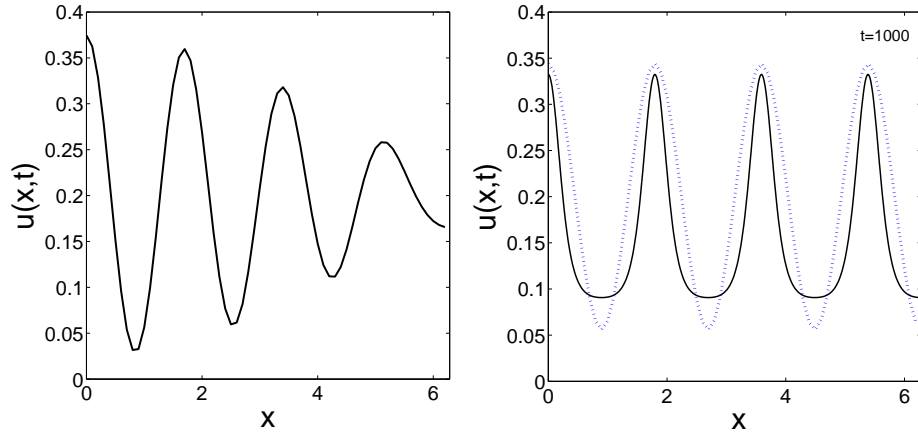


Fig. 3.8: Left: Initial condition $u = u_c + \varepsilon(\bar{A}_1 M_1 \cos(k_1 x) + \bar{A}_2 M_2 \cos(k_2 x))$ with $k_1 = 4$ and $k_2 = 3.5$, where $\bar{A}_1 = 0.144$, $\bar{A}_2 = 0.228$ is in the basin of attraction of the equilibrium $(0, A_2)$. Right: The comparison between the numerical solution of system (1.1)-(1.3) (solid line) and the expected solution (3.32).

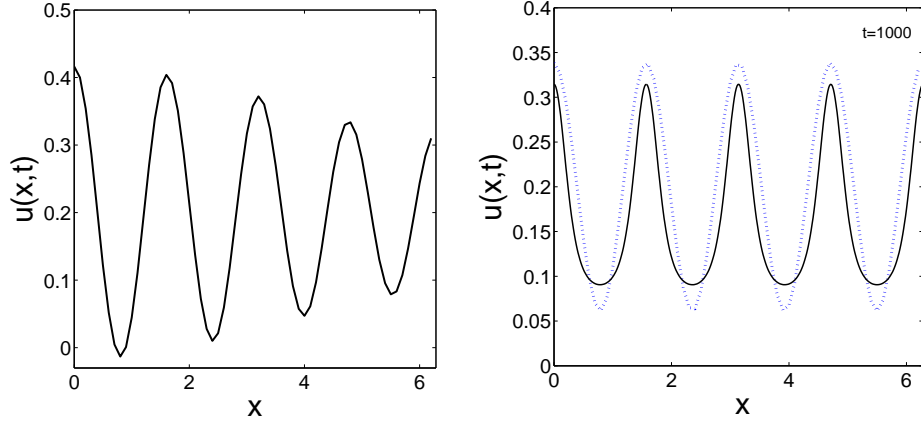


Fig. 3.9: Left: Initial condition $u = u_c + \varepsilon(\bar{A}_1 M_1 \cos(k_1 x) + \bar{A}_2 M_2 \cos(k_2 x))$ with $k_1 = 4$ and $k_2 = 3.5$, where $\bar{A}_1 = 0.344$, $\bar{A}_2 = 0.108$ is in the basin of attraction of the equilibrium $(A_1, 0)$. Right: The comparison between the numerical solution of system (1.1)-(1.3) (solid line) and the expected solution (3.33) (dashed line).

4 Conclutions

In this paper we have analyzed the pattern formation of a volume-filling chemotaxis model with the logistic cell growth. We have first established the sufficient conditions of destabilization for the uniform steady-state by local stability analysis. By deriving the cubic and the quintic Stuart-Landau equations near the instability threshold χ_c , we have studied the process of pattern formation for both the supercritical case and the subcritical case. For the case of multiple unstable modes, a competition model of two unstable modes has been obtained. Moreover, for the subcritical case, we have verify the existence of patterns with large amplitudes for $\chi < \chi_c$. This gives an affirmative answer to the open question proposed in [2].

All theoretical results have been tested against numerical solutions showing excellent qualitative and good quantitative agreement.

Inspired by the obtained results, we will further study the large amplitude patterns of the system (1.1), such as their structure and stability. In addition, the research idea in this paper can be applied to other biological models, such as the chemotaxis models with different kinetic terms and chemotactic flux introduced by Wang and Xu [7].

Appendix A Derivation of coefficient equations

Let

$$\mathbf{w} = \begin{pmatrix} W^{(1)} \\ W^{(2)} \end{pmatrix} = \begin{pmatrix} u - \bar{u} \\ v - \bar{v} \end{pmatrix},$$

and then (1.1) can be rewritten as

$$\mathbf{w}_t = \mathcal{L}^x \mathbf{w} + \mathcal{N}^x \mathbf{w}, \quad (\text{A.1})$$

where

$$\mathcal{L}^\chi = K + D^\chi \nabla^2, \\ \mathcal{N}\mathcal{L}^\chi \mathbf{w} = \begin{pmatrix} -\chi \nabla \left((1 - 2u_c) W^{(1)} \nabla W^{(2)} - (W^{(1)})^2 \nabla W^{(2)} \right) - \frac{\mu}{u_c} (W^{(1)})^2 \\ 0 \end{pmatrix}.$$

We expand χ , \mathbf{w} and t as follows

$$\begin{cases} \chi = \chi_c + \varepsilon \chi_1 + \varepsilon^2 \chi_2 + \varepsilon^3 \chi_3 + \varepsilon^4 \chi_4 + \varepsilon^5 \chi_5 + \dots, \\ \mathbf{w} = \varepsilon \mathbf{w}_1 + \varepsilon^2 \mathbf{w}_2 + \varepsilon^3 \mathbf{w}_3 + \varepsilon^4 \mathbf{w}_4 + \varepsilon^5 \mathbf{w}_5 + \dots, \\ t = t(T_1, T_2, T_3, \dots), \quad T_i = \varepsilon^i t, i = 1, 2, \dots \end{cases} \quad (\text{A.2})$$

and obtain

$$L^\chi = L^{\chi_c} - \varepsilon M_{\chi_1} \nabla^2 - \varepsilon^2 M_{\chi_2} \nabla^2 - \dots, \quad (\text{A.3})$$

where

$$M_{\chi_i} = \begin{pmatrix} 0 & \chi_i(u_c - u_c^2) \\ 0 & 0 \end{pmatrix}, \quad i = 1, 2, \dots.$$

Substituting (A.2) and (A.3) into (A.1) and collecting the terms at each order in ε , we obtain the following sequence of coefficient equations

$O(\varepsilon)$:

$$\mathcal{L}^{\chi_c} \mathbf{w}_1 = 0, \quad (\text{A.4})$$

$O(\varepsilon^2)$:

$$\mathcal{L}^{\chi_c} \mathbf{w}_2 = \mathbf{F}, \quad (\text{A.5})$$

$O(\varepsilon^3)$:

$$\mathcal{L}^{\chi_c} \mathbf{w}_3 = \mathbf{G}, \quad (\text{A.6})$$

$O(\varepsilon^4)$:

$$\mathcal{L}^{\chi_c} \mathbf{w}_4 = \mathbf{H}, \quad (\text{A.7})$$

$O(\varepsilon^5)$:

$$\mathcal{L}^{\chi_c} \mathbf{w}_5 = \mathbf{P}, \quad (\text{A.8})$$

where:

$$\begin{aligned} \mathbf{F} &= \frac{\partial \mathbf{w}_1}{\partial T_1} + M_{\chi_1} \nabla^2 \mathbf{w}_1 \\ &\quad + \chi_c (1 - 2u_c) \nabla \begin{pmatrix} W_1^{(1)} \nabla W_1^{(2)} \\ 0 \end{pmatrix} + \frac{\mu}{u_c} \begin{pmatrix} (W_1^{(1)})^2 \\ 0 \end{pmatrix}, \end{aligned} \quad (\text{A.9})$$

$$\begin{aligned} \mathbf{G} &= \frac{\partial \mathbf{w}_1}{\partial T_2} + \frac{\partial \mathbf{w}_2}{\partial T_1} + M_{\chi_1} \nabla^2 \mathbf{w}_2 + M_{\chi_2} \nabla^2 \mathbf{w}_1 + \frac{2\mu}{u_c} \begin{pmatrix} W_1^{(1)} W_2^{(1)} \\ 0 \end{pmatrix} \\ &\quad + \chi_c (1 - 2u_c) \nabla \begin{pmatrix} W_2^{(1)} \nabla W_1^{(2)} + W_1^{(1)} \nabla W_2^{(2)} \\ 0 \end{pmatrix} \\ &\quad - \chi_c \nabla \begin{pmatrix} (W_1^{(1)})^2 \nabla W_1^{(2)} \\ 0 \end{pmatrix} + \chi_1 (1 - 2u_c) \nabla \begin{pmatrix} W_1^{(1)} \nabla W_1^{(2)} \\ 0 \end{pmatrix}, \end{aligned} \quad (\text{A.10})$$

$$\begin{aligned} \mathbf{H} &= \frac{\partial \mathbf{w}_2}{\partial T_2} + \frac{\partial \mathbf{w}_1}{\partial T_3} + \frac{\partial \mathbf{w}_3}{\partial T_1} + M_{\chi_1} \nabla^2 \mathbf{w}_3 + M_{\chi_2} \nabla^2 \mathbf{w}_2 + M_{\chi_3} \nabla^2 \mathbf{w}_1 \\ &\quad + \chi_c (1 - 2u_c) \nabla \begin{pmatrix} W_1^{(1)} \nabla W_3^{(2)} + W_3^{(1)} \nabla W_1^{(2)} + W_2^{(1)} \nabla W_2^{(2)} \\ 0 \end{pmatrix} \end{aligned}$$

$$\begin{aligned}
& + \chi_1(1 - 2u_c) \nabla \left(\frac{W_1^{(1)} \nabla W_2^{(2)} + W_2^{(1)} \nabla W_1^{(2)}}{0} \right) \\
& + \chi_2(1 - 2u_c) \nabla \left(\frac{W_1^{(1)} \nabla W_1^{(2)}}{0} \right) \\
& - \chi_c \nabla \left(\frac{(W_1^{(1)})^2 \nabla W_2^{(2)} + 2W_1^{(1)} W_2^{(1)} \nabla W_1^{(2)}}{0} \right) \\
& - \chi_1 \nabla \left(\frac{(W_1^{(1)})^2 \nabla W_1^{(2)}}{0} \right) + \frac{\mu}{u_c} \left(\frac{(W_2^{(1)})^2 + 2W_1^{(1)} W_3^{(1)}}{0} \right), \quad (\text{A.11})
\end{aligned}$$

and

$$\begin{aligned}
\mathbf{P} = & \frac{\partial \mathbf{w}_1}{\partial T_4} + \frac{\partial \mathbf{w}_2}{\partial T_3} + \frac{\partial \mathbf{w}_3}{\partial T_2} + \frac{\partial \mathbf{w}_4}{\partial T_1} \\
& + M_{\chi_1} \nabla^2 \mathbf{w}_4 + M_{\chi_2} \nabla^2 \mathbf{w}_3 + M_{\chi_3} \nabla^2 \mathbf{w}_2 + M_{\chi_4} \nabla^2 \mathbf{w}_1 \\
& + \chi_c(1 - 2u_c) \nabla \left(\frac{W_1^{(1)} \nabla W_4^{(2)} + W_4^{(1)} \nabla W_1^{(2)}}{0} \right) \\
& + \chi_c(1 - 2u_c) \nabla \left(\frac{W_2^{(1)} \nabla W_3^{(2)} + W_3^{(1)} \nabla W_2^{(2)}}{0} \right) \\
& + \chi_1(1 - 2u_c) \nabla \left(\frac{W_2^{(1)} \nabla W_2^{(2)} + W_1^{(1)} \nabla W_3^{(2)} + W_3^{(1)} \nabla W_1^{(2)}}{0} \right) \\
& + \chi_2(1 - 2u_c) \nabla \left(\frac{W_1^{(1)} \nabla W_2^{(2)} + W_2^{(1)} \nabla W_1^{(2)}}{0} \right) \\
& + \chi_3(1 - 2u_c) \nabla \left(\frac{W_1^{(1)} \nabla W_1^{(2)}}{0} \right) \\
& - \chi_c \nabla \left(\frac{2W_1^{(1)} W_3^{(1)} \nabla W_1^{(2)} + 2W_1^{(1)} W_2^{(1)} \nabla W_2^{(2)}}{0} \right) \\
& - \chi_c \nabla \left(\frac{(W_1^{(1)})^2 \nabla W_3^{(2)} + (W_2^{(1)})^2 \nabla W_1^{(2)}}{0} \right) \\
& - \chi_1 \nabla \left(\frac{2W_1^{(1)} W_2^{(1)} \nabla W_1^{(2)} + (W_1^{(1)})^2 \nabla W_2^{(2)}}{0} \right) \\
& - \chi_2 \nabla \left(\frac{(W_1^{(1)})^2 \nabla W_1^{(2)}}{0} \right) + \frac{2\mu}{u_c} \left(\frac{W_2^{(1)} W_3^{(1)} + W_1^{(1)} W_4^{(1)}}{0} \right). \quad (\text{A.12})
\end{aligned}$$

Appendix B The cubic Stuart-Landau equation

Substituting \mathbf{w}_1 into (A.9) and combining $\chi_1 = \frac{\partial \mathbf{w}}{\partial T_1} = 0$ lead to

$$\mathbf{F} \triangleq \frac{1}{4} A^2 \sum_{i=0,2} F_i \cos(ik_c x), \quad (\text{B.1})$$

where

$$F_i = \left(\frac{\frac{2\mu M^2}{u_c}}{0} \right) - i^2 K_c^2 \left(\frac{M \chi_c (1 - 2u_c)}{0} \right), \quad i = 0, 2.$$

The solution of (A.5) with Neumann boundary condition is given by

$$\mathbf{w}_2 = A^2 \mathbf{w}_{20} + A^2 \mathbf{w}_{22} \cos(2k_c x). \quad (\text{B.2})$$

Substituting (B.2) into (A.5), we have

$$L_i \mathbf{w}_{2i} = \frac{1}{4} F_i, \quad L_i = K - i^2 K_c^2 D^{\chi_c}, \quad i = 0, 2. \quad (\text{B.3})$$

Further calculations deduce that \mathbf{w}_{20} , \mathbf{w}_{22} are given as in (3.16).

Substitute \mathbf{w}_1 , \mathbf{w}_2 and $\chi_1 = \frac{\partial \mathbf{w}}{\partial T_1} = 0$ into (A.10) and one have

$$\mathbf{G} = \left(\frac{dA}{dT_2} \rho - \mathbf{G}_{11} A + \mathbf{G}_{13} A^3 \right) \cos(k_c x) + A^3 \mathbf{G}_3 \cos(3k_c x), \quad (\text{B.4})$$

where

$$\begin{aligned} \mathbf{G}_{11} &= \begin{pmatrix} 0 & k_c^2 \chi_2 (u_c - u_c^2) \\ 0 & 0 \end{pmatrix} \rho = \begin{pmatrix} k_c^2 \chi_2 (u_c - u_c^2) \\ 0 \end{pmatrix}, \\ \mathbf{G}_{13} &= \begin{pmatrix} \chi_c (2u_c - 1) k_c^2 (W_{20}^{(1)} + MW_{22}^{(2)} - \frac{1}{2} W_{22}^{(1)}) \\ 0 \end{pmatrix} \\ &\quad + \begin{pmatrix} \frac{1}{4} \chi_c M^2 k_c^2 + \frac{\mu M}{u_c} (2W_{20}^{(1)} + W_{22}^{(1)}) \\ 0 \end{pmatrix}, \end{aligned}$$

and

$$\begin{aligned} \mathbf{G}_3 &= \begin{pmatrix} \chi_c (2u_c - 1) k_c^2 (3MW_{22}^{(2)} + \frac{3}{2} W_{22}^{(1)}) \\ 0 \end{pmatrix} \\ &\quad + \begin{pmatrix} \frac{3}{4} \chi_c M^2 k_c^2 + \frac{\mu}{u_c} MW_{22}^{(1)} \\ 0 \end{pmatrix}. \end{aligned}$$

By the solvability condition $\langle \mathbf{G}, \mathbf{w}^* \rangle = 0$ (the form of \mathbf{w}^* can be seen in (3.13)), we obtain the cubic Stuart-Landau equation (3.18) of amplitude A .

Appendix C The quintic Stuart-Landau equation

Combining with (B.4), the solution of (A.6) with Neumann boundary condition is given by

$$\mathbf{w}_3 = (A \mathbf{w}_{31} + A^3 \mathbf{w}_{32}) \cos(k_c x) + A^3 \mathbf{w}_{33} \cos(3k_c x), \quad (\text{C.1})$$

where \mathbf{w}_{31} , \mathbf{w}_{32} and \mathbf{w}_{33} satisfy

$$\begin{cases} L_1 \mathbf{w}_{31} = \sigma \rho - G_{11}, \\ L_1 \mathbf{w}_{32} = -L \rho + G_{13}, \\ L_3 \mathbf{w}_{33} = G_3 \end{cases} \quad (\text{C.2})$$

and $L_i, i = 1, 3$ are given in (B.3).

Substitute \mathbf{w}_1 , \mathbf{w}_2 and \mathbf{w}_3 into (A.11), take $\chi_1 = \frac{\partial \mathbf{w}}{\partial T_1} = 0$, and then

$$\begin{aligned} \mathbf{H} = & \left(\mathbf{w}_{20} \frac{\partial A^2}{\partial T_2} + H_{02} A^2 + H_{04} A^4 \right) + \left(\frac{\partial A}{\partial T_3} - k_c^2 M_{\chi_3} A \right) \rho \cos(k_c x) \\ & + \left(\mathbf{w}_{22} \frac{\partial A^2}{\partial T_2} + H_{22} A^2 + H_{24} A^4 \right) \cos(2k_c x) + H_4 A^4 \cos(4k_c x), \end{aligned}$$

where

$$\begin{aligned} H_{02} = & \frac{\mu M}{u_c} \begin{pmatrix} W_{31}^{(1)} \\ 0 \end{pmatrix}, \\ H_{04} = & \frac{\mu}{u_c} \begin{pmatrix} (W_{20}^{(1)})^2 + W_{32}^{(1)} M + \frac{1}{2} (W_{22}^{(1)})^2 \\ 0 \end{pmatrix}, \\ H_{22} = & -4k_c^2 M_{\chi_2} W_{22} + \frac{\mu M}{u_c} \begin{pmatrix} W_{31}^{(1)} \\ 0 \end{pmatrix} \\ & + (2u_c - 1)k_c^2 \begin{pmatrix} \chi_c W_{31}^{(1)} + \chi_c M W_{31}^{(2)} + \chi_2 M \\ 0 \end{pmatrix}, \\ H_{24} = & \chi_c (2u_c - 1)k_c^2 \begin{pmatrix} W_{32}^{(2)} M + 3W_{33}^{(2)} M + W_{32}^{(1)} \\ 0 \end{pmatrix} \\ & + \chi_c (2u_c - 1)k_c^2 \begin{pmatrix} 4W_{20}^{(1)} W_{22}^{(2)} - W_{33}^{(1)} \\ 0 \end{pmatrix} \\ & + 2\chi_c k_c^2 \begin{pmatrix} W_{22}^{(2)} M^2 + M W_{20}^{(1)} \\ 0 \end{pmatrix} \\ & + \frac{\mu}{u_c} \begin{pmatrix} 2W_{20}^{(1)} W_{22}^{(1)} + W_{32}^{(1)} M + W_{33}^{(1)} M \\ 0 \end{pmatrix}, \end{aligned}$$

and

$$\begin{aligned} H_4 = & \chi_c (2u_c - 1)k_c^2 \begin{pmatrix} 6W_{33}^{(2)} M + 2W_{33}^{(1)} + 4W_{22}^{(1)} W_{22}^{(2)} \\ 0 \end{pmatrix} \\ & + 2\chi_c k_c^2 \begin{pmatrix} W_{22}^{(2)} M^2 + M W_{22}^{(1)} \\ 0 \end{pmatrix} \\ & + \frac{\mu}{u_c} \begin{pmatrix} \frac{1}{2} (W_{22}^{(1)})^2 + W_{33}^{(1)} M \\ 0 \end{pmatrix}. \end{aligned}$$

By the solvability condition $\langle \mathbf{H}, \mathbf{w}^* \rangle = 0$, we obtain

$$\frac{\partial A}{\partial T_3} = \gamma A \quad \text{with } \gamma = \frac{k_c^2 \chi_3 (u_c - u_c^2) M^*}{1 + M M^*} > 0.$$

And then, A can not capture the evolution of the amplitude. So, we choose $\frac{\partial \mathbf{w}}{\partial T_3} = \chi_3 = 0$ simply to satisfy the solvability condition. Notice of (3.18), the expression \mathbf{H} can be rewritten as

$$\begin{aligned} \mathbf{H} = & ((2\sigma \mathbf{w}_{20} + H_{02}) A^2 + (H_{04} - 2L \mathbf{w}_{20}) A^4) \\ & + ((2\sigma \mathbf{w}_{22} + H_{22}) A^2 + (H_{24} - 2L \mathbf{w}_{22}) A^4) \cos(2k_c x) \end{aligned}$$

$$+ H_4 A^4 \cos(4k_c x).$$

It is easy to see that the solution of (A.7) with Neumann boundary condition is

$$\mathbf{w}_4 = A^2 \mathbf{w}_{40} + A^4 \mathbf{w}_{41} + (A^2 \mathbf{w}_{42} + A^4 \mathbf{w}_{43}) \cos(2k_c x) + A^4 \mathbf{w}_{44} \cos(4k_c x), \quad (\text{C.3})$$

where \mathbf{w}_{40} , \mathbf{w}_{41} , \mathbf{w}_{42} , \mathbf{w}_{43} and \mathbf{w}_{44} satisfy

$$\begin{cases} L_0 \mathbf{w}_{40} = 2\sigma \mathbf{w}_{20} + H_{02}, \\ L_0 \mathbf{w}_{41} = -2L \mathbf{w}_{20} + H_{04}, \\ L_2 \mathbf{w}_{42} = 2\sigma \mathbf{w}_{22} + H_{22}, \\ L_2 \mathbf{w}_{43} = -2L \mathbf{w}_{22} + H_{24}, \\ L_4 \mathbf{w}_{44} = H_4 \end{cases} \quad (\text{C.4})$$

and the definition of $L_i, i = 0, 2, 4$ are given in (B.3).

Substituting $\mathbf{w}_1, \mathbf{w}_2, \mathbf{w}_3, \mathbf{w}_4$ into (A.12) and combining $\chi_1 = \chi_3 = \frac{\partial \mathbf{w}}{\partial T_1} = \frac{\partial \mathbf{w}}{\partial T_3} = 0$ lead to

$$\begin{aligned} \mathbf{P} = & \left(\frac{\partial A}{\partial T_4} \rho + \frac{\partial A}{\partial T_2} \mathbf{w}_{31} + 3A^2 \frac{\partial A}{\partial T_2} \mathbf{w}_{32} \right. \\ & \left. - A \mathbf{P}_{11} + A^3 \mathbf{P}_{13} + A^5 \mathbf{P}_{15} \right) \cos(k_c x) + \mathbf{P}^*, \end{aligned}$$

where

$$\mathbf{P}_{11} = k_c^2 (M_{\chi_2} \mathbf{w}_{31} + M_{\chi_4} \rho),$$

$$\mathbf{P}_{13} = -k_c^2 M_{\chi_2} \mathbf{w}_{32}$$

$$\begin{aligned} & + (2u_c - 1) \chi_c k_c^2 \left(W_{40}^{(1)} + W_{20}^{(1)} W_{31}^{(2)} - \frac{1}{2} W_{22}^{(1)} W_{31}^{(2)} \right) \\ & + (2u_c - 1) \chi_c k_c^2 \left(W_{31}^{(1)} W_{22}^{(2)} + W_{42}^{(2)} M - \frac{1}{2} W_{42}^{(1)} \right) \\ & + (2u_c - 1) \chi_2 k_c^2 \left(W_{22}^{(2)} M + W_{20}^{(1)} - \frac{1}{2} W_{22}^{(1)} \right) \\ & + \frac{1}{4} \chi_c k_c^2 \left(2M W_{31}^{(1)} + W_{31}^{(2)} M^2 \right) + \frac{1}{4} \chi_2 k_c^2 M^2 \begin{pmatrix} 1 \\ 0 \end{pmatrix} \\ & + \frac{2\mu}{u_c} \left(W_{40}^{(1)} M + \frac{1}{2} W_{42}^{(1)} M + W_{20}^{(1)} W_{31}^{(1)} + \frac{1}{2} W_{22}^{(1)} W_{31}^{(1)} \right), \end{aligned}$$

$$\begin{aligned} \mathbf{P}_{15} = & (2u_c - 1) \chi_c k_c^2 \left(W_{41}^{(1)} + W_{20}^{(1)} W_{32}^{(2)} - \frac{1}{2} W_{22}^{(1)} W_{32}^{(2)} + W_{32}^{(1)} W_{22}^{(2)} \right) \\ & + (2u_c - 1) \chi_c k_c^2 \left(\frac{3}{2} W_{22}^{(1)} W_{33}^{(2)} - W_{33}^{(1)} W_{22}^{(2)} + W_{43}^{(2)} M - \frac{1}{2} W_{43}^{(1)} \right) \\ & + \chi_c k_c^2 \left(\frac{1}{2} M W_{32}^{(1)} - \frac{1}{2} M W_{33}^{(1)} + 2W_{20}^{(1)} W_{22}^{(2)} M + \frac{1}{4} W_{32}^{(2)} M^2 \right) \\ & + \chi_c k_c^2 \left(\frac{3}{4} W_{33}^{(2)} M^2 + (W_{20}^{(1)})^2 + \frac{1}{2} (W_{22}^{(1)})^2 - W_{20}^{(1)} W_{22}^{(1)} \right) \end{aligned}$$

$$+ \frac{2\mu}{u_c} \left(W_{41}^{(1)} M + \frac{1}{2} W_{43}^{(1)} M + W_{20}^{(1)} W_{32}^{(1)} + \frac{1}{2} W_{22}^{(1)} W_{32}^{(1)} + \frac{1}{2} W_{22}^{(1)} W_{33}^{(1)} \right)$$

and the expression of \mathbf{P}^* involves all terms orthogonal to \mathbf{w}^* . By solvability condition $\langle \mathbf{P}, \mathbf{w}^* \rangle = 0$, we obtain

$$\frac{\partial A}{\partial T_4} = \tilde{\sigma} A - \tilde{L} A^3 + \tilde{Q} A^5, \quad (\text{C.5})$$

where

$$\begin{cases} \tilde{\sigma} = \frac{\langle -\sigma \mathbf{w}_{31} + \mathbf{P}_{11}, \psi \rangle}{\langle \rho, \psi \rangle}, \\ \tilde{L} = \frac{\langle 3\sigma \mathbf{w}_{32} - L \mathbf{w}_{31} + \mathbf{P}_{13}, \psi \rangle}{\langle \rho, \psi \rangle}, \\ \tilde{Q} = \frac{\langle 3L \mathbf{w}_{32} - \mathbf{P}_{15}, \psi \rangle}{\langle \rho, \psi \rangle}. \end{cases} \quad (\text{C.6})$$

Adding up (C.5) to (3.18), we get the quintic Stuart-Landau equation (3.24) of amplitude A .

Appendix D Competition model

Substituting (3.29) into (A.9), we have

$$\begin{aligned} \mathbf{F} = & \sum_{l=1}^2 \left[\frac{\partial A_l}{\partial T_1} - k_l^2 \begin{pmatrix} 0 & \chi_1(u_c - u_c^2) \\ 0 & 0 \end{pmatrix} A_l \right] \rho_l \cos(k_l x) \\ & + F_{01} A_1^2 + F_{02} A_2^2 + F_{21} A_1^2 \cos(2k_1 x) + F_{22} A_2^2 \cos(2k_2 x) \\ & + F_p A_1 A_2 \cos(k_1 + k_2)x + F_m A_1 A_2 \cos(k_1 - k_2)x, \end{aligned}$$

where

$$\begin{aligned} F_{0i} &= \frac{\mu}{2u_c} \begin{pmatrix} M_i^2 \\ 0 \end{pmatrix}, \quad F_{2i} = \frac{\mu}{2u_c} \begin{pmatrix} M_i^2 \\ 0 \end{pmatrix} - k_i^2 \chi_c (1 - 2u_c) \begin{pmatrix} M_i \\ 0 \end{pmatrix}, \quad i = 1, 2, \\ F_p &= \frac{\mu}{u_c} M_1 M_2 \begin{pmatrix} 1 \\ 0 \end{pmatrix} + \frac{1}{2} (2u_c - 1) \chi_c \begin{pmatrix} k_2^2 M_1 + k_1^2 M_2 + k_1 k_2 M_1 + k_1 k_2 M_2 \\ 0 \end{pmatrix}, \\ F_m &= \frac{\mu}{u_c} M_1 M_2 \begin{pmatrix} 1 \\ 0 \end{pmatrix} + \frac{1}{2} (2u_c - 1) \chi_c \begin{pmatrix} k_2^2 M_1 + k_1^2 M_2 - k_1 k_2 M_1 - k_1 k_2 M_2 \\ 0 \end{pmatrix}. \end{aligned}$$

Similarly, we take $\chi_1 = \frac{\partial \mathbf{w}}{\partial T_1} = 0$ simply to satisfy the solvability condition. Then,

$$\begin{aligned} \mathbf{F} = & F_{01} A_1^2 + F_{02} A_2^2 + F_{21} A_1^2 \cos(2k_1 x) + F_{22} A_2^2 \cos(2k_2 x) \\ & + F_p A_1 A_2 \cos(k_1 + k_2)x + F_m A_1 A_2 \cos(k_1 - k_2)x \end{aligned} \quad (\text{D.1})$$

and the solution of (A.5) with Neumann boundary condition is given by

$$\begin{aligned} \mathbf{w}_2 = & \sum_{l=1}^2 A_l^2 \sum_{i=0,2} \mathbf{w}_{2i}^l \cos(ik_l x) \\ & + A_1 A_2 (\mathbf{w}_{2p} \cos(k_1 x + k_2 x) + \mathbf{w}_{2m} \cos(k_1 x - k_2 x)), \end{aligned} \quad (\text{D.2})$$

where \mathbf{w}_{20}^l , \mathbf{w}_{22}^l , \mathbf{w}_{2p} and \mathbf{w}_{2m} satisfy

$$\begin{cases} K\mathbf{w}_{20}^l = F_{0l}, \quad l = 1, 2, \\ (K - 4k_l^2 D^{\chi_c}) \mathbf{w}_{22}^l = F_{2l}, \quad l = 1, 2, \\ (K - (k_1 + k_2)^2 D^{\chi_x}) \mathbf{w}_{2p} = F_p, \\ (K - (k_1 - k_2)^2 D^{\chi_x}) \mathbf{w}_{2m} = F_m. \end{cases}$$

Substituting (3.29) and (D.2) into (A.10), and combining $\chi_1 = \frac{\partial \mathbf{w}}{\partial T_1} = 0$, we have

$$\mathbf{G} = \sum_{l=1}^2 \left(\frac{dA_l}{dT_2} \rho_l - A_l \mathbf{G}_{11}^l + A_l^3 \mathbf{G}_{13}^l + \frac{A_1^2 A_2^2}{A_l} \mathbf{G}_{12}^l \right) \cos(k_l x) + \mathbf{G}^*, \quad (\text{D.3})$$

where

$$\begin{aligned} \mathbf{G}_{11}^l &= M_{\chi_2} k_l^2 \rho_l, \\ \mathbf{G}_{13}^l &= (2u_c - 1) \chi_c k_l^2 \begin{pmatrix} W_{22}^{l(2)} M_l - \frac{1}{2} W_{22}^{l(1)} + W_{20}^{l(1)} \\ 0 \end{pmatrix} \\ &\quad + \frac{1}{4} \chi_c k_l^2 \begin{pmatrix} M_l^2 \\ 0 \end{pmatrix} + \frac{\mu}{u_c} M_l \begin{pmatrix} 2W_{20}^{l(1)} + W_{22}^{l(1)} \\ 0 \end{pmatrix}, \\ \mathbf{G}_{12}^1 &= \left(\frac{1}{2} (2u_c - 1) \chi_c ((k_1^2 + k_1 k_2) W_{2p}^{(2)} M_2 + (k_1^2 - k_1 k_2) W_{2m}^{(2)} M_2 \right. \\ &\quad \left. + k_1 k_2 (W_{2m}^{(1)} - W_{2p}^{(1)}) + 2W_{20}^{2(1)} k_1^2) + \frac{1}{2} \chi_c k_1^2 M_2^2 \right. \\ &\quad \left. + \frac{\mu}{u_c} (2W_{20}^{2(1)} M_1 + W_{2p}^{(1)} M_2 + W_{2m}^{(1)} M_2) \right) \begin{pmatrix} 1 \\ 0 \end{pmatrix}, \\ \mathbf{G}_{12}^2 &= \left(\frac{1}{2} (2u_c - 1) \chi_c ((k_2^2 + k_1 k_2) W_{2p}^{(2)} M_1 + (k_2^2 - k_1 k_2) W_{2m}^{(2)} M_1 \right. \\ &\quad \left. + k_1 k_2 (W_{2m}^{(1)} - W_{2p}^{(1)}) + 2W_{20}^{1(1)} k_2^2) + \frac{1}{2} \chi_c k_2^2 M_1^2 \right. \\ &\quad \left. + \frac{\mu}{u_c} (2W_{20}^{1(1)} M_2 + W_{2p}^{(1)} M_1 + W_{2m}^{(1)} M_1) \right) \begin{pmatrix} 1 \\ 0 \end{pmatrix}. \end{aligned}$$

By the solvability condition, we can obtain the competition model (3.30) of two unstable modes, where

$$\begin{aligned} \sigma_l &= \frac{\langle \mathbf{G}_{11}^l, \psi_l \rangle}{\langle \rho_l, \psi_l \rangle}, \quad L_l = \frac{\langle \mathbf{G}_{13}^l, \psi_l \rangle}{\langle \rho_l, \psi_l \rangle}, \quad \Omega_l = \frac{\langle \mathbf{G}_{12}^l, \psi_l \rangle}{\langle \rho_l, \psi_l \rangle}, \\ \psi_l &= \begin{pmatrix} M_l^* \\ 1 \end{pmatrix}, \quad M_l^* = \frac{\alpha}{\mu + k_l^2 d_1}, \quad l = 1, 2. \end{aligned}$$

References

- [1] M.J. Ma, C.H. Ou and Z.A. Wang, Stationary solutions of a volume-filling chemotaxis model with logistic growth and their stability, SIAM J. APPL. MATH., 72: 740-766, 2012.

- [2] M.J. Ma, J.J. Hu, J.C. Tao and C.Q. Tang, Non-existence of stationary pattern of a chemotaxis model with logistic growth, *Nonlinear Analysis*, 105: 3-9, 2014.
- [3] A.M. Turing. The chemical basis of morphogenesis, *Philos. Trans. R. Soc. Lond. B*, 273: 37-72, 1952.
- [4] T. Hillen and K. Painter, Global existence for a parabolic chemotaxis model with prevention of overcrowding, *Advances in Applied Mathematics*, 26: 280-301, 2001.
- [5] K. Painter and T. Hillen, Voluming-filling and quorum-sensing in models for chemosensitive movement, *Can. Appl. Math. Q.*, 10: 501-543, 2002.
- [6] T. Hillen and K.J. Painter, A user's guide to PDE models for chemotaxis, *J. Math. Biol.*, 58: 183-217, 2009.
- [7] X. Wang and Q. Xu, Spiky and transition layer steady states of chemotaxis systems via global bifurcation and Helly's compactness theorem, *J Math Biol*, 66: 1241-1266, 2013.
- [8] C. Ou and W. Yuan, Traveling Wavefronts in a Volume-Filling Chemotaxis Model, *SIAM J Appl Dyn Syst*, 8(1): 390-416, 2009.
- [9] M. Ma, D. Yang and H. Tang, Traveling fronts of the volume-filling chemotaxis model with general kinetics, *Applied Mathematics and Computation*, 216: 3162-3171, 2010.
- [10] Y. Han, Z. Li, S. Zhang and M. Ma, Wavefront invasion for a volume-filling chemotaxis model with logistic growth, *Computers and Mathematics with Applications*, 71: 471-478, 2016.
- [11] G. Gambino, M.C. Lombardo and M. Sammartino, Turing instability and pattern formation for the Lengyel-Epstein system with nonlinear diffusion, *Acta Appl Math*, 132: 283-294, 2014.
- [12] G. Gambino, M.C. Lombardo and M. Sammartino, Pattern formation driven by cross-diffusion in a 2D domain, *Nonlinear Analysis: Real World Applications*, 14: 1755-1779, 2013.
- [13] G. Gambino, M.C. Lombardo and M. Sammartino, Turing instability and traveling fronts for a nonlinear reaction-diffusion system with cross-diffusion, *Mathematics and Computers In Simulation*, 82: 1112-1132, 2012.
- [14] G. Gambino, M.C. Lombardo, M. Sammartino and V. Sciacca, Turing pattern formation in the Brusselator system with nonlinear diffusion, *Physical Review E*, 88: 042925, 2013.
- [15] M. van Hecke, P.C. Hohenberg and W. van Saarloos, Amplitude equations for pattern forming systems, *Fundamental Problems in Statistical Mechanics III*, Elsevier: North-Holland, Amsterdam, 1994, pp. 245-278.
- [16] R. Hoyle, *Pattern Formation. An Introduction to Method*, Cambridge University Press, Cambridge, 2006.

- [17] D.J. Wollkind, V.S. Manoranjan and L.Zhang, weakly nonlinear stability analyses of prototype reaction-diffusion model equations, *SIAM Rev.*, 36(2): 176-214, 1994.
- [18] L. Segel, *Modeling dynamic phenomena in molecular and cellular biology*, 2nd ed., Cambridge University Press, New York, 1987.